Nature Communications

https://doi.org/10.1038/s41467-026-69576-w

Article in Press

Developmental underpinnings of morphological disparity in the avian bony palate

Received: 31 July 2025

Accepted: 3 February 2026

Cite this article as: Plateau, O., Navalón, G., Benito, J. *et al.* Developmental underpinnings of morphological disparity in the avian bony palate. *Nat Commun* (2026). https://doi.org/10.1038/s41467-026-69576-w

Olivia Plateau, Guillermo Navalón, Juan Benito & Daniel J. Field

Developmental underpinnings of morphological disparity in the avian bony palate

Olivia Plateau[1,2,3*], Guillermo Navalón[1,4], Juan Benito[1], Daniel J. Field[1,5*]

[1] Department of Earth Sciences, University of Cambridge, Downing Street, Cambridge CB2 3EQ, United Kingdom

[2]The Institute of Ecology and Evolution, University of Bern, Baltzerstrasse, Bern 63012, Switzerland

[3]Naturhistorisches Museum Bern, Bernastrasse 15, Bern 3005, Switzerland

[4]Departamento de Ciencias de la Vida, Universidad de Alcalá, Alcalá de Henares, Madrid, 28805, Spain.

[5]Museum of Zoology, University of Cambridge, Downing Street, Cambridge CB2 3EJ, United Kingdom

*Emails for correspondence: olivia.plateau@unibe.ch; djf70@cam.ac.uk

Abstract

The bony palate of palaeognaths was long thought to retain the plesiomorphic condition for crown birds, but recent fossil evidence suggests that aspects of palaeognath palate morphology are derived from a neognath-like ancestral state. Relatedly, heterochronic shifts have been proposed as the mechanism underpinning major evolutionary transitions in avian palate morphology, but this hypothesis has never been explicitly tested with a broad phylogenetic assessment of morphological variation through avian ontogeny. Here, we assess palatal changes through post-hatching ontogeny across the major extant avian subclades and find that although palaeognaths exhibit distinct ontogenetic changes relative to neognaths, no signatures of heterochrony underlie these developmental differences. However, we find that important patterns of morphological change appear to be dictated by variation in developmental mode. Our results clarify the ontogenetic mechanisms driving avian palate disparity and illustrate the influence of developmental mode on evolvability of a key morphofunctional system in the avian skull.

Introduction

The deepest phylogenetic divergence within crown birds, between palaeognaths (ratites and tinamous) and neognaths (all other birds), was originally recognised on the basis of the morphology of the skull's pterygoid-palatinum complex (hereafter, PPC)[1–4]. The PPC is composed of five bones: an unpaired vomer and paired palatines and pterygoids. Whereas palaeognaths exhibit a fused, immobile contact between the pterygoid and palatine, the PPC of neognaths is characterised by a mobile joint between these elements, enabling an enhanced degree of palatal kinesis[1,4,5].

Multiple aspects of palaeognath morphology, including their distinctive PPCs, have been hypothesised to reflect the retention of the ancestral crown bird condition[6–9]. By contrast, certain authors have suggested that the apparently plesiomorphic aspects of the palaeognath PPC may in fact be derived, reflecting a hypothesised paedomorphic developmental shift[10,11] from a neognath-like ancestral condition associated with the loss of flight[12–14]. Towards reconciling these alternative views, the PPC morphologies of Mesozoic avialans (i.e., *Archaeopteryx, Gobipteryx* and *Hesperornis*) have been investigated to illuminate the nature of the PPC along the crownward portion of the avian stem lineage. Early investigations[15] concluded that the PPCs of Palaeognathae share more similarities with those of Mesozoic stem birds than with Neognathae, bolstering the hypothesis that palaeognaths retain a more plesiomorphic arrangement of the palate than neognaths. However, unanticipated paleontological discoveries have recently contributed additional nuance to this debate, with new specimens of Mesozoic near-crown stem birds recognised as exhibiting mobile PPC arrangements similar to those of some neognaths [16–19].

Despite the potential importance of these palaeontological findings, to date they lack formal corroboration from developmental datasets beyond investigations limited to a narrow phylogenetic sample [20,21]. Here, we investigate post-hatching ontogeny of the PPC complex across a broad range of extant birds (family-level representation across Palaeognathae and members of all major neognath subclades[22]; Fig. 1) to clarify the developmental and evolutionary underpinnings of morphological variation in the avian PPC. As the vomer is often reduced and vestigial in neognaths [23–27], we focus on morphological variation of the palatine and the

pterygoid. We use landmark-based three-dimensional geometric morphometrics (Fig.2) to quantify morphological changes in the PPC throughout ontogeny and assess morphological variation within and among major clades to assess the main ontogenetic drivers of morphological variation between Palaeognathae and Neognathae. These data provide unprecedented insight into the nature of morphological variation in the avian PPC and clarify patterns of evolutionary change in the PPC near the origin of crown birds.

Results

Quantifying morphological disparity among major bird clades

We compared macroevolutionary and ontogenetic variation in PPC morphology among major clades (Fig. 1, Supplementary Figure 1) of extant birds in two ways: 1) treating the PPC as a single complex, and 2) examining shape variation of the pterygoid and palatine as individual elements.

When considering the PPC as a single complex, the morphospace defined by the first two PCs accounts for 52% of PPC shape variation (Fig. 3). The negative end of PC1 is associated with anteroposteriorly short but mediolaterally wide palatines combined with antero-posteriorly elongate pterygoids bearing a mediolaterally broad and robust quadrate articulation, whereas the positive end of PC1 captures anteroposteriorly elongate palatines with anteroposteriorly short pterygoids (Fig. 3A). The negative end of PC2 is associated with anteroposteriorly elongate palatines and pterygoids, whereas the positive end of PC2 captures anteroposteriorly short but mediolaterally wide palatines combined with anteroposteriorly short pterygoids (Fig. 3A).

Palaeognathae and Neognathae are differentiated along PC1 (Fig. 3A-B), with palaeognaths exhibiting considerably greater morphological disparity than neognaths (Fig. 3C), including several of the most divergent PPC morphologies among extant birds (Fig. 3D; Supplementary Figure 2 and 3; Supplementary Data 1 and 2). While the palatines of some palaeognaths (i.e. ostrich and the tinamou *Crypturellus*) are anteroposteriorly elongate and mediolaterally narrow, others (i.e. emu, rhea, and the tinamou *Nothoprocta*) are much shorter and wider. In contrast, whereas the pterygoids of emu, ostriches and rheas are anteroposteriorly short and mediolaterally broad, those of tinamous are elongate and tube-shaped.

Within Neognathae, the subclades Strisores (nightbirds) and Telluraves (landbirds) exhibit the greatest range of morphological disparity, and in some cases overlap with palaeognaths along PC1 and PC2 (Fig. 3B-C). However, these instances of overlap (Fig. 3A) are restricted to a small handful of neognaths (7 species out of 70) with especially derived cranial and PPC morphologies (adult parrots, toucans, hornbills and frogmouths, and both immature and adult tropicbirds), all of which exhibit relatively short palatines and extremely wide pterygoids. Certain divergent palaeognath morphologies also result in overlap with neognaths along PC1 and PC2; for instance, the adult ostrich overlaps with Galloanserae (land- and waterfowl; Fig. 3A-B).

Nonetheless, all neognath subclades exhibit substantial overlap along PC1-PC2 (see SI, Supplementary Note 1). Although pairwise distances are relatively low among neognath subclades, statistically significant morphological differences distinguish Galloanserae, Strisores, Phaethoquornithes and Telluraves from other subclades (Fig. 3C-D; Supplementary Figure 2 and 3; Supplementary Data 1 and 2).

Analysing the palatine and pterygoid as individual elements (Fig. 4) yields similar general patterns along PC1and PC2 to those from our analyses of the PPC as a single complex. Collectively, the first two principal components account for 46% of total shape variation for the palatine (Fig. 4A), and 78% for the pterygoid (Fig. 4B). Furthermore, geometric dissimilarity between the pterygoids of Palaeognathae and Neognathae is greater than that for the palatines (Fig. 5). In contrast, within Neognathae, palatine shape is more distinct among major clades than the pterygoid, especially among Anseriformes, Mirandornithes and Charadriiformes, and between Telluraves and Strisores (Fig. 5).

Dividing our total sample into immature and adult subsets reveals patterns of morphological disparity that are broadly similar to those of the combined dataset (Supplementary Figure 4,5; Supplementary Data 3). However, both in terms of within-clade morphological disparity and among-clade pairwise distances, immature palaeognaths are more morphologically variable than adults are. In contrast, most neognath adults are more disparate than immatures are (Supplementary Figure 4,5; Supplementary Data 3). Nevertheless, differences among clades in the whole dataset are greater than those in the separate immature and adult subsets. The immature and adult subsamples exhibit comparable phylogenetic signal, with only slight variation in *Kmult* (Immature: K = 0.78, P = 0.001; Adult: K = 0.83, P = 0.001).

Ontogenetic trajectories across avian phylogeny

To compare ontogenetic variation within and among major extant bird clades (Fig. 1), we calculated angles between the ontogenetic shape trajectories of each species and estimated the degree of ontogenetic divergence (i.e. individuals becoming less similar throughout ontogeny) *versus* convergence (i.e. individuals becoming more similar throughout ontogeny) of each pair of species based on pairwise Procrustes distances between immature and adult individuals (see Methods). To identify heterochronic shifts in ontogenetic variation among groups (i.e. changes in the rate and timing of developmental processes[28]), hypothesised as a driver of the distinct palate morphologies of Palaeognathae and Neognathae[11], we applied a multi-test approach comparing size-shape relationships among major clades (see Methods).

Group-specific shape differences in ontogenetic trajectories

Within Palaeognathae, comparisons of the angle of ontogenetic trajectories show a bimodal distribution (Fig. 6), with a cluster of taxa around 100° (the tinamou *Nothoprocta* vs. all other palaeognaths), and a second cluster around 60° (comparisons among all other palaeognaths). Neognaths exhibit a greater range of differences in ontogenetic trajectories, (31° - 137°), with a continuous distribution of values between the extremes represented by the trajectories of *Recurvirostra avosetta* vs *Plegadis falcinellus* and *Falco tinnunculus* vs *Spheniscus demersus*. (Fig. 5A). When Palaeognathae and Neognathae are compared, angles among ontogenetic trajectories exhibit a continuous distribution from 60° (*Perdix perdix* vs *Dromaius novaehollandiae*) to 137° (*Crypturellus tataupa* compared vs *Plegadis falcinellus*) (Fig. 6, Supplementary Data 4).

Within the major subclades comprising Neognathae, comparisons within Galloanserae exhibit a narrower range of variation (between 37°, when comparing *Dendrocygna arborea* to *Malacorhynchus membranaceus*, to 117°, when comparing *Anas platyrhynchos* to *Numida meleagris*), and a more heterogeneous distribution of values than comparisons within Neoaves (Fig. 6). The greater disparity observed in Neoaves is largely attributable to variation within the hyperdiverse subclade Telluraves, which range from 33° (*Anorrhinus galeritus* vs *Pteroglossus viridis*) to 127° (*Falco tinnunculus* vs *Falco naumanni*). Other neognath subclades occupy essentially the full range of variation between the extremes delimited by Palaeognathae and Telluraves (see Supplementary Note 2 for more details). Between clades, however, a broad

spectrum of variation in ontogenetic trajectories is evident, with almost uniform variation between 31° and 137° (Fig. 6). Except for especially high values of intraclade variation in Telluraves, the most extreme differences are restricted to interclade comparisons rather than arising from intraclade comparisons.

Ontogenetic shape divergence and convergence among birds

Within most major extant bird subclades, we find a general pattern in which the PPC morphologies of different species diverge throughout ontogeny (Fig. 7); that is, immatures of different species exhibit comparatively similar PPC morphologies, whereas adults are more geometrically distinct (although see Supplementary Note 2 for more details). This pattern is further exaggerated in Telluraves, which exhibit the greatest degree of within-clade ontogenetic shape divergence (Fig. 7; Supplementary Data 5). Notably, Anseriformes exhibit the opposite pattern, with interspecific PPC morphology converging throughout ontogeny (Fig. 7), while Galliformes show more ontogenetic divergence than Anseriformes (see Supplementary Note 2 for more details).

Among major neognath subclades, PPC shape tends to diverge throughout ontogeny. By contrast, palaeognath PPC morphology converges towards adult neognath PPC morphology as ontogeny progresses (Fig. 7, Supplementary Figure 6), in accordance with our finding that differences in the shape of the PPC between palaeognaths and neognaths are greatest at early ontogenetic stages (Supplementary Figure 4). These morphological differences are more pronounced in the pterygoid than in the palatine (Supplementary Figure 4).

Non-heterochronic ontogenetic variation in the PPCs of Palaeognathae and Neognathae

Based on model comparisons (see Materials and Methods), we found that comparisons of ontogenetic trajectories between Palaeognathae and Neognathae were the most effective basis for testing heterochronic hypotheses for the full PPC complex as well as for the palatine in isolation (Table 1; Supplementary Figure 7A,B). However, for the pterygoid, the most informative model for testing for heterochrony instead involved comparing ontogenetic allometries between Palaeognathae and the major subgroups of Neognathae (Table 1; Supplementary Figure 7C).

For both the isolated palatine and the PPC complex, palaeognath allometric ontogenetic slopes differ significantly from Neognathae (Table 1; Supplementary Figure 7A,B; Supplementary Data

6). Non-heterochronic processes appear to underlie ontogenetic changes between palaeognaths and neognaths (Table 1;Supplementary Data 6, Thf2: significant), and their trajectories tend to converge[29,30] as post-hatching ontogeny progresses (Table 1; Supplementary Figure 7A,B) as adults show a great degree of morphological similarity than immatures. For the pterygoid, excluding the comparison between Palaeognathae and Galliformes (see below), allometric ontogenetic slopes of Palaeognathae also significantly differ from those of Neognathae (Table 1; Supplementary Figure 7C, Supplementary Data 6). Furthermore, these trajectories also differ in shape trajectory (Table 1; Supplementary Data 6, Thf2: significant)) and their ontogenetic shape trajectories tend to converge towards each other during post-hatching ontogeny (Table 1; Supplementary Figure 7C). While ontogenetic allometric trajectories between Palaeognathae and Galliformes show no differences in slope, their intercepts are significantly different (Table 1; Supplementary Data 6, Thf1: significant), indicating parallel slopes, rather than heterochronic variations from a common ancestral ontogenetic allometric trend. Overall, our results illustrate a general lack of evidence for heterochronic changes giving rise to the morphological differences in the PPCs of Palaeognathae and Neognathae (see SI, Supplementary Note 1, 2 for more details).

Influence of developmental mode on ontogenetic variation in the avian PPC

Finally, we interrogated how variation in PPC ontogenetic trajectories is shaped by variation in life history strategies along the altricial-precocial spectrum[31](Fig. 8). This provides an additional exploration of the macroevolutionary effects of developmental variation beyond linear relationships between size and shape across ontogenies. Across extant birds we found a continuous range of variation describing ontogenetic divergence and convergence and note that altricial taxa exhibit markedly greater degrees of ontogenetic divergence than precocial taxa (Fig. 8; Supplementary Data7). To statistically assess the relationship between life history traits and ontogenetic variation (changes in PPC shape and morphospace trajectory), we assessed the correlation between our ontogenetic parameters (morphological distance, angles between ontogenetic trajectories, and *Divergence-Convergence* values) and a semi-continuous quantitative index of avian developmental mode[32]. The resultant Ordinary Least Squares linear models (Fig. 9; Supplementary Data 8) revealed weak but significant correlations between all variables (i.e., Distance: R^2 = 0.11, P = *0.024*; Angle: R^2 = 0.08, P = *0.044*; *Divergence –*

Convergence: $R^2 = 0.14$, P = *0.07*) that became non-significant when phylogenetic relationships were controlled for (Fig. 9B). This pattern (i.e., OLS significant, PGLS non-significant) may indicate that shifts in PPC ontogenetic variables and developmental mode both occurred early in the evolutionary history of crown birds (Clauss et al., 2013, Fig. 9), at the base of large clades and not within these subclades (Fig. 9).

Discussion

Our study represents the most detailed quantitative exploration of avian PPC ontogeny to date and fills an important gap in our understanding of avian palate evolution.

We found no evidence for signatures of heterochronic processes (that is, evolutionary changes in the rate and timing of developmental changes) contributing to the differentiation of diagnostic palate morphologies of Palaeognathae and Neognathae, in agreement with more limited previous explorations[20,21,33,34]. Previous work suggested that differences between Palaeognathae and Neognathae emerge early in pre-hatching development, and at no stage do palaeognaths resemble earlier developmental stages of neognaths[21,32,33]. Together with our results, these observations suggest that neither pre- nor post-hatching ontogenetic changes support a heterochronic origin of the palaeognath PPC.

By contrast, we found evidence that variation in developmental mode plays a prominent role in influencing PPC ontogeny across avian diversity. Specifically, precocial birds tend to exhibit convergent morphological trajectories of the PPC throughout ontogeny, whereas the PPCs of altricial groups tend to diverge as ontogeny progresses (Fig.8). These results mirror patterns from other anatomical modules across the avian body[35], and suggest that developmental mode variation may modulate the strength of constraints on PPC morphology at macroevolutionary scales.

Moreover, our results suggest that major shifts in developmental mode and correlated large-scale patterns in PPC ontogenetic trajectories occurred only a limited number of times, early in the evolutionary histories of major crown bird clades, complicating straightforward inferences regarding PPC morphology in the ancestral crown bird from extant taxa. Our results hint at an evolutionary scenario in which rapid evolutionary changes in developmental mode in the early

Cenozoic were associated with major evolutionary changes in PPC morphology, overprinting plesiomorphic morphological signatures.

Clear morphological differences in the PPC between Palaeognathae and Neognathae are discernible from analyses of both individual PPC components and the entire complex. In all versions of our analyses, Palaeognathae shows greater morphological disparity than all the major clades within Neognathae. Individually, the pterygoid shows a greater degree of morphological differentiation between these two major clades than the palatine, reflecting a notable degree of constraint on the pterygoid morphology of neognaths and a lack thereof in palaeognaths.

These interclade patterns reflect fundamental differences in the configuration and function of the avian palate. We hypothesise that the fusion and loss of mobility between the palatine and the pterygoid in Palaeognathae[2,36] may have released ancestral functional constraints associated with cranial kinesis, allowing these bones to vary more freely. This effect may have been less pronounced in the palatine than in the pterygoid due to the palatine's immobile connections with the rostrally positioned premaxilla and the laterally placed maxilla (and, when present, the medially positioned vomer [24–26]). By contrast, in all prokinetic birds the pterygoid articulates only at mobile joints (with the palatine rostrally and the quadrate caudally)[2,4,25,37,38].

Within Neognathae, the morphology of the pterygoid is remarkably conservative, presumably related to the maintenance of its key prokinetic role within this clade as a force-transmitting lever between the quadrate and palatine. By contrast, the palatine is considerably more variable, with Strisores (nightbirds) and Telluraves (landbirds) exhibiting the greatest levels of morphological disparity in the palatine, in line with these clades exhibiting some of the most extreme rostral morphologies among extant birds[39–41]. Given that the major components of the rostrum appear to ossify at relatively similar stages of development[21,33,34,42,43], we suggest that the palatine may be more affected by adaptive changes in rostral morphology than the pterygoid, which warrants future investigation in studies of avian pre- and post-hatching cranial development and function.

This hypothesis may also be supported by myological evidence. Previous investigations have highlighted the impact of muscle arrangement on the skull shape of other vertebrates, such as mammals[44,45]. Although these relationships are considerably less well-studied in birds, the *musculus pterygoideus* (*Dorsalis* and *Ventralis*) and the *musculus protractor pterygoidei et quadrati*[37] are associated with avian beak opening and closing, connecting the palatine to the

pterygoid, and the pterygoid to the quadrate, respectively[2]. The arrangement of these muscles is relatively simple in Palaeognathae[37,46,47] and more complex in Neognathae, with numerous muscle subdivisions increasing the number of muscle-bone contacts[48–50,37]. The more complex muscular attachments associated with the neognath pterygoid may be related to its comparatively constrained degree of morphological disparity relative to that of palaeognaths, and also relative to the neognath palatine.

Notably, some neognaths overlap with palaeognaths along the main axes describing PPC geometry, such as some parrots (Psittaciformes), frogmouths (Strisores: Podargidae), hornbills (Bucerotiformes), and toucans (Piciformes: Ramphastidae). This pattern appears to be driven primarily by palatine morphology rather than by the pterygoid (Fig.3A, Fig.4A-B), as these taxa generally exhibit short but extremely wide palatines, a condition widespread in Palaeognathae. Importantly, these taxa include an array of neognaths with secondarily reduced palatal kinesis (e.g., toucans[51]), as well as hyperkinetic taxa with divergent rostral morphologies (e.g., parrots[52]), suggesting that multiple factors may be responsible for these convergent shifts in different clades.

We note that limitations of current morphometric tools represent a major challenge to quantifying what is perhaps the most fundamental cranial distinction between palaeognaths and neognaths: the fused connection between the pterygoid and palatine of palaeognaths[1–3,36]. For instance, the general arrangement of the palatine and pterygoid in the frogmouth *Podargus strigoides* is strikingly similar to that of palaeognaths (note overlapping PPC geometries along PC1 and PC2 in Fig. 3A and Fig. 4A,B). However, even though the anterior articular surface of the pterygoid sits atop the dorsal surface of the caudal palatine in *Podargus*, these elements remain unfused, unlike the condition in Palaeognathae where these elements fuse to one-another.

Clade-specific differences in palate morphology are already apparent at the hatchling stage in most bird lineages. For instance, differences in form between palaeognath and neognath PPCs and pterygoids are even more pronounced among hatchlings than adults. Whereas palaeognaths exhibit their greatest degree of morphological disparity in the PPC at the hatchling stage, neognaths (with the exception of Anseriformes) exhibit greater disparity at the adult stage than at the hatchling stage (see Supplementary Note 3 for a more detailed discussion). It is worth noting that species-specific differences in palate morphology are likely present as well. For example,

Nothoprocta exhibits an ontogenetic trajectory along PC1 that is opposite to that of the other palaeognaths examined (Fig. 3; see Supplementary Note 3 for additional details). Although a detailed examination of such species-level differences falls outside the scope of the present study, these patterns highlight the potential value of future research based on a more extensive dataset, both in terms of species sampling and representation of ontogenetic stages.

The direction of ontogenetic change for each species was captured by the trajectory angle as well as by divergence/convergence outcomes. Notably, the opposite trajectory observed in *Nothoprocta* occurs only along PC1, which accounts for approximately 39% of total shape variance and partly reflects size-related differences between the palatine and pterygoid.

The patterns we observe appear to be dictated in part by variation in developmental mode. Specifically, in precocial and super precocial[31,53] taxa (e.g., all palaeognaths, anseriforms) a great deal of ossification and morphological change occurs during pre-hatchling development. By contrast, altricial and super altricial[31,53] taxa (all of which are neognaths) generally hatch in a comparatively weakly ossified state, in which interactions between muscle action and extensively unossified skeletal elements can induce pronounced variation in bone morphology during post-hatching growth[35]. Galliformes, the precocial and super precocial sister taxon to Anseriformes, represent a notable exception to this pattern, exhibiting the lowest observed values of morphological disparity at both stages. This observation is in line with the generally conservative cranial morphology of galliforms[54], hinting at additional clade-specific developmental constraints[43] responsible for canalising galliform cranial morphology that are worthy of further investigation. Crucially, only Neoaves experience post-hatching palatal segmentation (see Online Methods), which is absent in Palaeognathae, and incomplete or absent in Galloanserae[24,36,55,56], yet the role played by this ontogenetic transformation in shaping palatal morphology remains uncertain.

Whereas altricial taxa tend to exhibit divergent ontogenetic trajectories of PPC morphology, and precocial taxa exhibit convergent trajectories (Fig.8), semi-altricial and semi-precocial taxa tend to exhibit intermediate values that are challenging to fully disentangle. This recalls broader macroevolutionary patterns among birds and other vertebrates, where clear ecomorphological patterns may only be discernible at the extremes of ecological variation, in which stronger selective pressures yield consistent morphological solutions. For instance, beak shape—a well-

studied aspect of avian skull variation—is distinct among taxa exhibiting highly distinct ecologies, but otherwise exhibits extensive overlap in form[57,58].

Previous studies have reported evidence for the contribution of heterochronic processes to craniofacial evolution near the origin of modern birds[59–61] and within major lineages such as Strisores[40]. However, our results suggest limited evidence for heterochrony as a major driver of morphological divergence in the avian PPC, emphasising that inferred macroevolutionary patterns in ontogenetic allometry may differ not only among anatomical elements but also in line with the phylogenetic scale under investigation [62–64].

Though long challenging to investigate quantitatively[32], previous research has illustrated the influence of the precocial-altricial spectrum on patterns of variation across the avian crown group, influencing biological parameters as varied as genomic evolutionary mode[65] and anatomical modules such as the legs[35], brain[66], and beak[57,58]. Collectively, these studies and our results suggest that the evolutionary emergence of avian altricial development was associated with an increase in morphological evolvability, perhaps representing a key innovation contributing to the striking imbalance of diversity and disparity of form that distinguishes precocial and altricial bird taxa in the present day. The underappreciated influence of developmental mode variation on macroevolutionary shifts in skeletal form highlights the need for further research into the evolutionary origins of avian altriciality and its phenotypic consequences.

Methods

Sampling, and 3D Data acquisition

To quantify morphological variation in the Pterygoid-Palatinium Complex of extant birds, we sampled species of all major bird lineages and grouped them following major clades in the Prum et al., 2015 phylogeny [Palaeognathae (n=5), Galliformes (n= 6), Anseriformes (n= 8), Strisores (n= 5), Columbaves (n= 3), Gruiformes (n= 3), Mirandornithes and Charadriiformes (n= 8), Phaethoquornithes (n= 16) and Telluraves + Hoatzin (Inopinaves, n= 16). One immature and one adult were sampled for a total of 70 extant bird species (Supplementary Data 9). Although data on absolute ontogenetic age is often missing from museum species, we sampled specimens as close as possible to the hatching stage based on size, plumage characteristics and the state of

skull bone fusion[27]. For some Palaeognathae, specimens treated as adults in our analyses were necessarily represented by subadults whose skull shape and size are almost identical to those of adults (see Supplementary Data 9). In some cases, we were unable to sample adult specimens of the same species as the corresponding immature specimen; for these taxa, we selected an adult from the same genus whose skull shape and size were closest to the original species (see Supplementary Data 9). We acknowledge the limitation of focusing on only two specific developmental stages, a necessary consequence of the difficulty of obtaining comparable material across such a broad representation of avian phylogenetic diversity. However, because our analyses target general patterns of ontogenetic variation at a broad phylogenetic scale, we consider it unlikely that this limitation substantially affects our conclusions.

Specimens collected for this study were obtained from the University of Cambridge Museum of Zoology (UMZC), the Natural History Museum (NHMUK), Tring, the Natural History Museum of Fribourg (NHMF), and the Natural History Museum of Bern (NMBE). These specimens were scanned at the Cambridge Biotomography Centre using a Nikon XTEK H 225 ST MicroCT scanner (μCT). Specimens from Fribourg and Bern were scanned using a Bruker Skyscan 2211 at the Geoscience Department of the University of Fribourg, Switzerland Scans of other species were downloaded from the online repository MorphoSource (https://www.morphosource.org/; see Supplementary Data 9 for a detailed list of specimens).

All 3D reconstructions of the bones of the PPC were obtained from image stacks using Avizo 2019.3 (Thermo Fisher Scientific). Due to extreme bone fusion in some adult specimens (e.g., *Pelecanus philippensis* and *Pteroglossus viridis*), the suture between the rostral portion of the palatine and the surrounding bones (i.e, premaxillary and maxillary) was not always clearly visible. For these specimens, we segmented the rostral portion of the palatine bone based on variation in bone porosity and density and used immature specimens as a reference as their palate bones remained unfused (see Supplementary Figure 8).

Because the vomer was reduced or vestigial (n = 2) or even absent (n = 17) in 19 species in our sample, we decided not to include this element in our dataset. As the palatine and pterygoid are key elements influencing the biomechanics of cranial kinesis[2], we decided to maximise ecological diversity by sampling as many species as possible, which would have been precluded had vomer been included.

During ontogeny, neoavian pterygoids undergo a process of division, named 'pterygoid segmentation[55], resulting in the generation of a transient independent hemipterygoid positioned between the palatine and pterygoid in immature specimens. The hemipterygoid then fuses with the caudal end of the palatine in adults[24,55,56,67]. To guarantee comparison between homologous structures, we defined the adult condition, where the hemipterygoid is completely fused to the palatine, as the reference morphology for our analyses. Therefore, for each immature specimen, the hemipterygoid was considered as part of the palatine and included in the palatine landmark scheme (see below for more details). In immature and adult Anseriformes, the anterior region of the pterygoid bears a pronounced rostral process, which may be homologous with the unsegmented hemipterygoid of immature Neoaves. Therefore, this region of the anseriform pterygoid was treated as part of the palatine, as for the neoavian hemipterygoid.

Three-dimensional Geometric Morphometrics

As the palatine and pterygoid articulate in intact bird skulls, characterising the shape of the full PPC could be disrupted by bone displacements, especially in osteological preparations of specimens. This is a greater potential risk for immature specimens, where bones are not yet in contact due to ongoing ossification. To enable accurate quantification of the full PPC, we followed the approach of Thomas et al., 2023 to generate 'data blocks' by landmarking each bone independently and combining these data blocks by scaling the shape configuration for specimen comparisons [68–70].

The PPC is a bilaterally symmetrical complex with paired palatines and pterygoids. We were primarily interested in comparisons of the morphology of the palatine with the pterygoid, and as such only focused on one side of the PPC (the left). For species whose left PPC elements were missing or damaged, we mirrored the corresponding bone from the right side using Blender (version 3.6).

A set of six anatomical landmarks and eight curves were digitized on the 3D meshes of the palatine, as well as six anatomical landmarks and nine curves on 3D meshes of the pterygoid (see Fig. 2 and SI, Supplementary Table 1). All landmarks were manually placed using the software Stratovan Checkpoint, and the curve semi-landmarks situated between landmarks were resampled following previous protocols [71] (Divet et al. 2016, see Supplementary Information for relevant code). Sliding (minimising bending energy) and Generalized Procrustes Analysis

(GPA),were carried out in the R statistical environment (version 4.4.0) using morphoBlocks (version 0.1.0) [70] (Thomas et al., 2021, see Code Availability section).

Multivariate and phylogenetic analysis

All multivariate and phylogenetic comparative analyses were conducted in the R statistical environment [72]. For details regarding code, see Code Availability section.

Morphological variation of the PPC

To explore morphological variation of the PPC, we conducted a principal components analysis (PCA) (see Figs. 3 and 4; Supplementary Figure 5, Supplementary Data 10) on each bone independently, and of the complex as a whole.

To estimate morphological disparity in each clade (see above), we calculated Procrustes variance using the *morphol.disparity* function (Geomorph R package (version 4.0.1) [68]). High values of Procrustes variance indicate high morphological disparity according to the whole landmark conformation of the entire sample. To test for differences in PPC morphology between clades, we performed a Procrustes ANOVA using *procD.lm* in the geomorph R package (version 4.0.1) [68]. Then, to assess which clades exhibited significant shape differences, we performed pairwise comparisons using the *pairwise* function from the RRPP R package[73], where a greater pairwise distance value indicates a greater degree of morphological differentiation between two groups. These tests were conducted on the bony complex as a whole (see Fig. 3) and on each individual bone (see Supplementary Figure 4).

To evaluate whether PPC morphology is correlated with phylogeny, we estimated phylogenetic signal of our Procrustes shape variables, using the *physignal* function in the geomorph R package (version 4.0.1) [68]. Phylogenetic signal was estimated separately on immature and adult specimens.

Ontogenetic trajectories of the PPC

Morphological variation during ontogeny is strongly associated with size changes[74]. Therefore, most ontogenetic studies to date have focused on the extent to which shape variation is correlated with size variation (i.e. ontogenetic allometry[30,63,64]). Because our results showed that allometry explained only a small portion of the variation in our data (Supplementary Data 6), we did not

undertake further analyses correcting for allometry. To compare ontogenetic trajectories and patterns within and between all major bird clades investigated, we computed three ontogenetic parameters. All ontogenetic parameters were calculated based on total morphological variability by directly comparing the landmark dataset after Procrustes superimposition (GPA). First, we extracted Euclidean distances between immature and adult specimens of each species as an estimate of the amount of morphological change during ontogeny. Second, because an ontogenetic trajectory can be defined as a vector between the immature and the adult of the same species, we quantified differences in ontogenetic trajectories by comparing vector angles between each species (see Supplementary Figure 9). We calculated two sets of angles: within groups and between groups. In the case of angles within a group, we calculated the angle between the vectors of each species within that group (i.e. all the coloured lines in Fig. 6: black, red, blue, etc.). As such, for n species, we calculate a total of $((n \times (n - 1)) / 2)$ angles. For instance, within Palaeognathae, we sampled five species: *Dromaius novaehollandiae*, *Rhea americana*, *Struthio camelus*, *Crypturellus tataupa*, and *Nothoprocta perdicaria*. For these, we first computed all the angles between the vector of *Dromaius* and those of the other four species (i.e. four angles). Then we calculated the angles between *Rhea* and the remaining species not yet compared (i.e. three angles), and so on. As a result, in the end, we obtained a total of ten angles within Paleognathae, reflecting five pairwise comparisons. In the case of angles between groups, we calculated the angles in the same manner, but between species from different groups instead (i.e. all the grey lines in Fig. 6). For example, we calculated all angles between the vectors of all palaeognath species and all the species within Neognathae. This approach allowed us to examine and illustrate the differences in ontogenetic trajectories occurring between groups. We computed angles using the dot product method commonly used to extract this metric between two vectors[75,76]. As a result, the greater the angle between ontogenetic vectors, the greater the difference between ontogenetic trajectories. Third, as angle measurements do not reveal whether the ontogenetic trajectories between two species are divergent (i.e. shape differences between the adults of different species are more different than shape differences between immatures) or convergent (i.e. the opposite case), we estimated divergence and convergence between ontogenetic trajectories (see Supplementary Figure 9). For each pair of species, we first calculated the Euclidean distance between immatures (d_1) and between adults (d_2), then subtracted the adult-to-immature distance ($d_{1\text{-}2} = d_1 - d_2$) (see Supplementary Figure 9). If $d_{1\text{-}2} > 0$,

the shape differences among the adults are less different than the shape differences among the immatures, indicating a case of convergence; By contrast, if $d_{1\text{-}2} < 0$, the shape differences among the adults are more different than those of the immatures, indicating a case of divergence. If $d_{1\text{-}2} \sim 0$, the ontogenetic trajectories can be considered more or less parallel, indicating a lack of both ontogenetic convergence and divergence. Similar to the approach followed for the angle comparisons, divergence/convergence calculations were performed both within groups and between groups, following the same colour coding. The resulting values are shown as frequency plots, displaying how often each value occurs across the dataset (Fig. 7).

Heterochronic tests

We analyzed evolutionary changes in ontogenetic trajectories following the framework proposed by Alberch et al., 1979[74], which has since has been widely applied across various phylogenetic groups including squamates[29,30,77], birds[40], non-avian dinosaurs[78], and mammals[79]. This approach focuses on examining the relationship between shape and size changes throughout ontogeny. Differences in these relationships across taxa therefore provide evidence for, and allow us to distinguish between, different heterochronic and non-heterochronic mechanisms shaping ontogenetic differences throughout the evolutionary history of a clade.

Because we lack statistical power to evaluate these relationships between individual species (species-level ontogenies are only represented by one immature and one adult individual in our sample) we sought to provide insight into signatures of the evolution of ontogenies manifesting at higher taxonomic levels by evaluating these relationships at the clade level [30]. We repeated this set of analyses for the whole PPC complex, as well as for the pterygoid and palatine in isolation.

To evaluate which linear models best explained variation in our morphometric datasets (i.e., Paleognathae vs Neognathae or Paleognathae vs all the Neognathae subgroups), we evaluated the relative fit of different allometric models (see Supplementary Figure 7) by using the R function 'model-comparison' in the RRPP package (version 2.1.2.999)[80]. We used the -likelihoods and penalty parameters to compare these models, and performed all downstream tests using the model with the lowest log-likelihood.

To evaluate whether different clades exhibit similar allometries we performed a Homogeneity of Slopes test using the 'procD.lm' and 'anova' functions in the geomorph[68] and RRPP packages (version 2.1.2.999)[80]. When 'procD.lm' yielded significant results, indicating differences in allometric slopes, we ran the 'Het2' test function[30] (see detailed function in Ollonen et al., 2024) to test whether the two groups being compared exhibit evidence of neoteny/acceleration (i.e. no difference in slopes) or whether the trajectories are convergent or divergent (i.e. significant differences between slopes).

When the results of 'procD.lm' were not significant, we performed a test of homogeneity of intercepts called 'Het1'[30] (see detailed function in Ollonen et al., 2024) to test whether the slopes of the two groups under comparison overlap (non-significant p-value) or not (significant p-value). In the event that the slopes do not overlap, it can be concluded that the slopes are parallel. However, if the slopes overlap, we used the peram.test [30] (see detailed function in Ollon et al., 2024) to test whether the morphology of the adults between the two groups differ (significant p-value) or not (non-significant p-value). If the results are significant, they suggest the presence of post-displacement, progenesis/hypermorphosis, pre-displacement, or neomorphic ontogenetic change, depending on the relationship between the two slopes.

Phylogenetic context of PPC ontogeny

To test the correlation between developmental mode and ontogenetic parameters (see above), we used a time-calibrated phylogeny from previously published trees[39]. We pruned the original 9,993 species in the original phylogeny[39] to match our 70-species sample using the R package *ape*(version 5.8)[81]. To follow the most up-to-date hypothesis of Palaeognathae phylogeny, we modified the tree topology for the group[22] on our backbone phylogeny.

To compare ontogenetic trajectories within a phylogenetic framework, we needed to estimate a single value per species for the angle and divergence/convergence values. Thus, we first estimated a reference ontogenetic trajectory against which to compare all our species. To do so, we used *gm.prcomp* to reconstruct the ancestral PPC shape for crown group birds (i.e. the last common ancestor of Palaeognathae and Neognathae). To reconstruct ancestral ontogenetic trajectories, we estimated an immature ancestral shape using only immature specimens, and an adult ancestral shape, using only adult specimens (supplementary Data 11). Then, we calculated angles and divergence/convergence values between the hypothetical ancestral ontogeny and

descendant ontogenies[40]. These new angles and divergence/convergence values were used to test the relationship between ontogenetic parameters and developmental mode (see below).

To characterise variation in avian developmental patterns, Ducatez and Field (2021)[32] conducted several PCoA analyses on qualitative traits used to assess developmental mode[31,53]. We used the chick PC scores (ChickPC1 and ChickPC2) from Ducatez and Field (2021)[32] as a quantitative estimate of developmental mode along the altricial - precocial spectrum.

Next, we used the phytools (version 2.4-4) R[82] package to estimate ancestral states for each ontogenetic variable (Chick PC1, ontogenetic distances, angles, and divergence/convergence values) and visualized them on the phylogeny with contMap, applying a maximum-likelihood approach for ancestral state estimation. To quantify patterns of ontogenetic trajectories, we conducted ordinary least squares (OLS) regressions of ontogenetic parameters and developmental mode using procD.lm in geomorph[68]. We tested whether ontogenetic distances, angles, and divergence/converge values were correlated with developmental mode, then conducted similar regressions within a phylogenetic comparative framework using phylogenetic generalized least-squares (PGLS) using procD.lm in geomorph[68].

Data Availability

The 3D models and landmark data generated in this study have been deposited on Figshare (https://doi.org/10.6084/m9.figshare.29618981). All other data generated in this study (e.g., PC scores, angles, and dataset information) are provided in the Supplementary Information. Source data are provided with this paper.

Code Availability

The R code used to analyse the data generated in this study has been deposited on Figshare (https://doi.org/10.6084/m9.figshare.29618981).

References

1. Huxley, T. H. On the classification of birds: and on the taxonomic value of the modifications of certain of the cranial bones observed in that class. *Proceedings of the Zoological Society of London* **27**, 415–472 (1867).
2. Bock, W. J. Kinetics of the avian skull. *Journal of Morphology* **114**, 1–42 (1964).
3. Gussekloo, S. W. & Zweers, G. A. The paleognathous pterygoid-palatinum complex. A true character? *Netherlands journal of zoology* **49**, 29–43 (1999).
4. Gussekloo, S. W., Vosselman, M. G. & Bout, R. G. Three-dimensional kinematics of skeletal elements in avian prokinetic and rhynchokinetic skulls determined by Roentgen stereophotogrammetry. *Journal of Experimental Biology* **204**, 1735–1744 (2001).
5. Zusi, R. L. Patterns of diversity in the avian skull. in *The skull* vol. 2 391–437 (University of Chicago Press, 1993).
6. Cracraft, J. Phylogeny and evolution of the ratite birds. *Ibis* **116**, 494–521 (1974).
7. Paton, T., Haddrath, O. & Baker, A. J. Complete mitochondrial DNA genome sequences show that modern birds are not descended from transitional shorebirds. *Proceedings of the Royal Society of London. Series B: Biological Sciences* **269**, 839–846 (2002).
8. Gibb, G. C., Kardailsky, O., Kimball, R. T., Braun, E. L. & Penny, D. Mitochondrial genomes and avian phylogeny: complex characters and resolvability without explosive radiations. *Molecular biology and evolution* **24**, 269–280 (2007).
9. Livezey, B. C. & Zusi, R. L. Higher-order phylogeny of modern birds (Theropoda, Aves: Neornithes) based on comparative anatomy. II. Analysis and discussion. *Zoological Journal of the Linnean Society* **149**, 1–95 (2007).
10. Dawson, A. Neoteny and the thyroid in ratites. *Reviews of Reproduction* **1**, 78–81 (1996).

11. Dawson, A., McNaughton, F. J., Goldsmith, A. R. & Degen, A. A. Ratite-like neoteny induced by neonatal thyroidectomy of European starlings, Sturnus vulgaris. *Journal of Zoology* **232**, 633–639 (1994).
12. De Beer, S. G. The evolution of ratites. *British Museum (Natural History) Bulletin (Zoological Series)* **4**, 59–70 (1956).
13. Gingerich, P. D. Evolutionary significance of the Mesozoic toothed birds. *Smithsonian Contributions to Paleobiology* **27**, 23–33 (1976).
14. Härlid, A. & Arnason, U. Analyses of mitochondrial DNA nest ratite birds within the Neognathae: supporting a neotenous origin of ratite morphological characters. *Proceedings of the Royal Society of London. Series B: Biological Sciences* **266**, 305–309 (1999).
15. Witmer, L. M. & Martin, L. D. The primitive features of the avian palate, with special reference to Mesozoic birds. *Travaux et Documents des Laboratoires de Géologie de Lyon* **99**, 21–40 (1987).
16. Torres, C. R., Norell, M. A. & Clarke, J. A. Bird neurocranial and body mass evolution across the end-Cretaceous mass extinction: The avian brain shape left other dinosaurs behind. *Science Advances* **7**, 1–9 (2021).
17. Benito, J., Kuo, P.-C., Widrig, K. E., Jagt, J. W. M. & Field, D. J. Cretaceous ornithurine supports a neognathous crown bird ancestor. *Nature* **611**, 100–105 (2022).
18. Benito J., Kuo P.C., Torres C.R., Navalón G., Plateau O., Clark A.D., Steell EM., Field J.D. Shouldering the challenge of deciphering avian palate evolution. *PNAS*, 1, 1-4 (2025).
19. Field, D., Burton, M. G., Benito, J., Plateau, O. & Navalón, G. Whence the birds: 200 years of dinosaurs, avian antecedents. *Biology Letters* **21**, 1–13 (2025).
20. Gussekloo, S. W. & Bout, R. G. Non-neotenous origin of the palaeognathous (Aves) pterygoid palate complex. *Canadian journal of zoology* **80**, 1491–1497 (2002).

21. Maxwell, E. E. Comparative ossification and development of the skull in palaeognathous birds (Aves: Palaeognathae). *Zoological Journal of the Linnean Society* **156**, 184–200 (2009).

22. Prum, R. O. *et al.* A comprehensive phylogeny of birds (Aves) using targeted next-generation DNA sequencing. *Nature* **526**, 569–573 (2015).

23. Jollie, M. Comments on the phylogeny and skull of the Passeriformes. *The Auk* **75**, 26–35 (1958).

24. Zusi, R. L. & Livezey, B. C. Variation in the os palatinum and its structural relation to the palatum osseum of birds (Aves). *Annals of Carnegie Museum* **75**, 137–180 (2006).

25. Gussekloo, S. W. *et al.* Functional and evolutionary consequences of cranial fenestration in birds. *Evolution* **71**, 1327–1338 (2017).

26. Hu, H. *et al.* Evolution of the vomer and its implications for cranial kinesis in Paraves. *Proceedings of the National Academy of Sciences* **116**, 19571–19578 (2019).

27. Plateau, O. & Foth, C. Common patterns of skull bone fusion and their potential to discriminate different ontogenetic stages in extant birds. *Frontiers in Ecology and Evolution* **9**, 1–15 (2021).

28. Gould, S. J. *Ontogeny and Phylogeny*. (Harvard University Press, 1977).

29. Esquerre, D., Sherratt, E. & Keogh, J. S. Evolution of extreme ontogenetic allometric diversity and heterochrony in pythons, a clade of giant and dwarf snakes. *Evolution* **71**, 2829–2844 (2017).

30. Ollonen, J. *et al.* Dynamic evolutionary interplay between ontogenetic skull patterning and whole-head integration. *Nature Ecology & Evolution* **8**, 536–551 (2024).

31. Starck, J. M. & Ricklefs, R. E. *Avian Growth and Development: Evolution within the Altricial-Precocial Spectrum*. (Oxford University Press, 1998).

32. Ducatez, S. & Field, D. J. Disentangling the avian altricial-precocial spectrum: Quantitative assessment of developmental mode, phylogenetic signal, and dimensionality. *Evolution* **75**, 2717–2735 (2021).

33. Maxwell, E. E. Comparative embryonic development of the skeleton of the domestic turkey (Meleagris gallopavo) and other galliform birds. *Zoology* **111**, 242–57 (2008).

34. Maxwell, E. E., Harrison, L. B. & Larsson, H. C. Assessing the phylogenetic utility of sequence heterochrony: evolution of avian ossification sequences as a case study. *Zoology* **113**, 57–66 (2010).

35. Botelho, J. F., Smith-Paredes, D. & Vargas, A. O. Altriciality and the Evolution of Toe Orientation in Birds. *Evolutionary Biology* **42**, 502–510 (2015).

36. McDowell, S. The bony palate of birds. Part I. The Palaeognathae. *The Auk* **65**, 520–549 (1948).

37. Baumel, J. J. & Witmer, L. M. *Nomina Anatomica Avium*. (Publications of the Nuttall Ornithological Club, Cambridge, MA, 1993).

38. Olsen, A. M. & Westneat, M. W. Linkage mechanisms in the vertebrate skull: Structure and function of three-dimensional, parallel transmission systems. *Journal of Morphology* **277**, 1570–1583 (2016).

39. Cooney, C. R. *et al.* Mega-evolutionary dynamics of the adaptive radiation of birds. *Nature* **542**, 344–347 (2017).

40. Navalon, G. *et al.* Craniofacial development illuminates the evolution of nightbirds (Strisores). *Proc Biol Sci* **288**, 1–10 (2021).

41. Navalon, G., Marugan-Lobon, J., Bright, J. A., Cooney, C. R. & Rayfield, E. J. The consequences of craniofacial integration for the adaptive radiations of Darwin's finches and Hawaiian honeycreepers. *Nat Ecol Evol* **4**, 270–278 (2020).

42. Arnaout, B., Lantigua, K. E., MacKenzie, E. M., McKinnell, I. W. & Maddin, H. C. Development of the chicken skull: A complement to the external staging table of Hamburger and Hamilton. *Anat Rec (Hoboken)* **304**, 2726–2740 (2021).

43. Arnaout, B., Brzezinski, K., Chen, A., Steventon, B. & Field, D. Comparative osteogenesis of galloanseran crania challenges assumptions of von Baer's Laws. Preprint at https://doi.org/10.21203/rs.3.rs-6606234/v1 (2025).

44. Fabre, A. C. *et al.* Do Muscles Constrain Skull Shape Evolution in Strepsirrhines? *The Anatomial Records* **301**, 291–310 (2018).

45. Brassard, C., Wertani, L., Herrel, A. & Jerbi, H. Variability of jaw muscles in Tunisian street dogs and adaptation to skull shape. *The Anatomical Record* 1–20 (2025).

46. George, J. C. & Berger, A. J. *Avian Myology*. (Academic Press, 1966).

47. Picasso, M. B. J., Mosto, C. & Tudisca, A. M. The feeding apparatus of Rhea americana (Aves, Palaeognathae): Jaw myology and ontogenetic allometry. *J Morphol* **284**, 1–13 (2023).

48. Zusi, R. L. The role of the depressor mandibulae muscle in kinesis of the avian skull. *Proceedings of the United States National Museum* **123**, 1–28 (1967).

49. Bhattacharyya, B. N. Diversity of feeding adaptations in certain columbid birds: A functional morphological approach. *Journal of Biosciences* **19**, 415–427 (1994).

50. Bhattacharyya, B. N. Avian Jaw Function: Adaptation of the Seven–Muscle System and a Review. *Proceedings of the Zoological Society* **66**, 75–85 (2013).

51. Höfling, E. & Gasc, J. P. Biomechanics of the skull and the bill in Ramphastos (Ramphastidae, Aves). II. Analysis of the conditions of movement of the bill. *Gegenbaurs Morphologisches Jahrbuch* **130**, 235–262 (1984).

52. Young, M. W. *et al.* The dual function of prokinesis in the feeding and locomotor systems of parrots. *Journal of Experimental Biology* **226**, jeb246659 (2023).

53. Starck, J. M. Evolution of avian ontogenies. in *Current Ornithology* vol. 10 275–366 (Springer New York, 1993).

54. Linde-Medina, M. Testing the cranial evolutionary allometric 'rule'in Galliformes. *Journal of Evolutionary Biology* **29**, 1873–1878 (2016).

55. Pycraft, W. P. Some points in the morphology of the palate of the Neognathæ. *Zoological Journal of the Linnean Society* **28**, 343–357 (1901).

56. Parker, W. K. VII. On the Structure and Development of the Bird's Skull. *Transactions of the Linnean Society of London* **1**, 99–154 (1876).

57. Bright, J. A., Marugan-Lobon, J., Cobb, S. N. & Rayfield, E. J. The shapes of bird beaks are highly controlled by nondietary factors. *Proceedings of the National Academy of Sciences* **113**, 1–15 (2016).

58. Navalón, G., Bright, J. A., Marugán-Lobón, J. & Rayfield, E. J. The evolutionary relationship among beak shape, mechanical advantage, and feeding ecology in modern birds. *Evolution* **73**, 422–435 (2019).

59. Bhullar, B.-A. S. *et al.* Birds have paedomorphic dinosaur skulls. *Nature* **487**, 223–226 (2012).

60. Fabbri, M. *et al.* The skull roof tracks the brain during the evolution and development of reptiles including birds. *Nature Ecology & Evolution* **1**, 1543–1550 (2017).

61. Beyrand, V. *et al.* Multiphase progenetic development shaped the brain of flying archosaurs. *Scientific Reports* **9**, 1–15 (2019).

62. Chatterji, R. M., Hipsley, C. A., Sherratt, E., Hutchinson, M. N. & Jones, M. E. H. Ontogenetic allometry underlies trophic diversity in sea turtles (Chelonioidea). *Evolutionary Ecology* **36**, 511–540 (2022).

63. Lanzetti, A., Coombs, E. J., Portela Miguez, R., Fernandez, V. & Goswami, A. The ontogeny of asymmetry in echolocating whales. *Proceedings of the Royal Society B* **289**, 1–9 (2022).

64. Le Verger, K. *et al.* Pervasive cranial allometry at different anatomical scales and variational levels in extant armadillos. *Evolution* **78**, 423–441 (2024).

65. Berv, J. S. *et al.* Genome and life-history evolution link bird diversification to the end-Cretaceous mass extinction. *Science Advances* **10**, 1–15 (2024).

66. Griesser, M., Drobniak, S. M., Graber, S. M. & van Schaik, C. P. Parental provisioning drives brain size in birds. *Proceedings of the National Academy of Sciences* **120**, 1:10 (2023).

67. Elzanowski, A. New observations on the skull of Hesperornis with reconstructions of the bony palate and otic region. *Postilla* **207**, 1–20 (1991).

68. Adams, D. C. & Otárola-Castillo, E. geomorph: an R package for the collection and analysis of geometric morphometric shape data. *Methods in ecology and evolution* **4**, 393–399 (2013).

69. Collyer, M. L., Davis, M. A. & Adams, D. C. Making heads or tails of combined landmark configurations in geometric morphometric data. *Evolutionary Biology* **47**, 193–205 (2020).

70. Thomas, D. B. *et al.* Constructing a multiple-part morphospace using a multiblock method. *Methods in Ecology and Evolution* **14**, 65–76 (2023).

71. Botton-Divet, L., Cornette, R., Fabre, A.-C., Herrel, A. & Houssaye, A. Morphological analysis of long bones in semi-aquatic mustelids and their terrestrial relatives. *Integrative and Comparative Biology* **56**, 1298–1309 (2016).

72. R Core Team. *R: A Language and Environment for Statistical Computing*. (Foundation for Statistical Computing, 2024).

73. Collyer, M. L. & Adams, D. C. RRPP: An r package for fitting linear models to high-dimensional data using residual randomization. *Methods in Ecology and Evolution* **9**, 1772–1779 (2018).

74. Alberch, P., Gould, S. J., Oster, G. F. & Wake, D. B. Size and shape in ontogeny and phylogeny. *Paleobiology* **5**, 296–317 (1979).

75. Sheets, H. D. & Zelditch, M. L. Studying ontogenetic trajectories using resampling methods and landmark data. *Hystrix* **24**, 1–67 (2013).

76. Foth, C., Hedrick, B. P. & Ezcurra, M. D. Cranial ontogenetic variation in early saurischians and the role of heterochrony in the diversification of predatory dinosaurs. *PeerJ* **4**, 1–41 (2016).

77. Piras, P. *et al.* The role of post-natal ontogeny in the evolution of phenotypic diversity in Podarcis lizards. *Journal of Evolutionary Biology* **24**, 2705–2720 (2011).

78. Fabbri, M. *et al.* A shift in ontogenetic timing produced the unique sauropod skull. *Evolution* **75**, 819–831 (2021).

79. White, H. E. *et al.* Pedomorphosis in the ancestry of marsupial mammals. *Current Biology* **33**, 2136–2150 (2023).

80. Collyer, M. L. & Adams, D. C. RRPP: An r package for fitting linear models to high-dimensional data using residual randomization. *Methods in Ecology and Evolution* **9**, 1772–1779 (2018).

81. Paradis, E., Claude, J. & Strimmer, K. APE: analyses of phylogenetics and evolution in R language. *Bioinformatics* **20**, 289–290 (2004).

82. Revell, L. J. phytools: an R package for phylogenetic comparative biology (and other things). *Methods in ecology and evolution* 217–223 (2012).

Acknowledgements

We are indebted to Matt Lowe (UMZC) and Judith White (NHM) for assistance with specimens, and Keturah Smithson (Cambridge Biotomography Centre) for CT scanning assistance. We would like to thank Michel Beaud and Boris Baeriswyl (Musée d'Histoire Naturelle Fribourg), Manuel Schweizer and Reto Hagmann (Naturhistorisches Museum Bern) for giving access to specimens and Sharon Grant for giving access to MorphoSource specimens. We thank Annabel Hunt (Cambridge) for insight into hemipterygoid homology guiding our landmark applications. We would like to thank the anonymous reviewers for their critical evaluation of our work, which enabled us to significantly improve our manuscript. This work was funded by UKRI grant MR/X015130/1 (D.J.F) and the SNSF grant P500PN_214284 (O.P). For the purpose of open access, the authors have applied a Creative Commons Attribution (CC BY) licence to any Author Accepted Manuscript version arising.

Author Contributions Statement

O.P. and D.J.F. conceived and designed the project. O.P. performed digital segmentation of the bones; designed the analytical framework with input from J.B. and conducted the geometric morphometric analyses with input from G.N.; O.P. designed the figures and wrote the original manuscript with input from all the authors (G.N., J.B., D.J.F.). O.P. and G.N. collected part of the dataset, while D.J.F. collected and curated the remaining data. O.P and D.J.F. secured funding for the project.

Competing Interests Statement

The authors declare no competing interests.

Tables (one single table)

Palaeognath palate morphology is unlikely to be neotenic. Results of the statistical test used to assess the presence of different heterochronic and/or non-heterochronic mechanisms that have shaped ontogenetic differences throughout the evolutionary history of a clade. Tests were conducted to identify differences between Palaeognathae and Neognathae in the complex (palatine + pterygoid), the palatine, and the pterygoid. Heterochronic results for all subgroups of Neognathae and Palaeognathae are presented in Supplementary Data 6. We followed the analytical framework described in Ollonen et al. (2024)[30]. We used the procD.lm function from the R package geomorph[68] to test homogeneity of slopes. We then used the procD.lm function from the R package geomorph[68] to test the homogeneity of slopes. Following Ollonen et al. (2024)[30], we performed a test of homogeneity of intercepts ('Het1') and a peram.test to assess whether adult morphology differs between the two groups. When procD.lm yielded significant results, we subsequently applied the 'Het2' test to determine whether the groups exhibit evidence of neoteny/acceleration or whether their ontogenetic trajectories are convergent/divergent (see detailed description in Ollonen et al., 2024[30]).

Test of Homogeneity of slopes							
procD.lm(coords ~ size * spp)							
Complex	**DF**	**SS**	**MS**	**Rsq**	**F**	**Z**	**Pr(>F)**
size	1,000	0,209	0,209	0,024	3,660	2,466	*0,0047**
spp (PavsNeo)	1,000	1,169	1,169	0,135	20,498	4,321	*0,0001**
size:spp	1,000	0,230	0,230	0,027	4,040	2,662	*0,0036**
Palatine							
size	1,0000	0,1677	0,1677	0,0311	4,4125	3,2058	*0,0006**
spp (PavsNeo)	1,0000	0,4153	0,4153	0,0769	10,9276	4,5877	*0,0001**
size:spp	1,0000	0,1057	0,1057	0,0196	2,7800	2,1952	*0,0140**
Pterygoid							
size	1,0000	0,2550	0,2550	0,0778	14,1950	3,1273	*0,0001**
spp (PavsNeo)	1,0000	0,6477	0,6477	0,1976	36,0617	3,7940	*0,0001**
size:spp	1,0000	0,1482	0,1482	0,0452	8,2526	2,7604	*0,0007**

Heterochrony test II (TfH2). Differences in shape trajectory		
Complex	**obs.diff**	**p.value**
	6,491998	0,002*
Palatine	**obs.diff**	**p.value**
	4,279724	*0,002**

Pterygoid	obs.diff	p.value
	1,161147	*0,002**

Figure Legends/Captions (for main text figures) listed in the order from 1 to 9

Figure 1. The pterygoid-palatinum complex (PPC) across bird phylogeny. A) Ontogenetic comparative morphology of the palatine and pterygoid of the primary extant bird clades investigated. For each group (colour-coded and numbered) we illustrate the cranium of an immature and an adult specimen in ventral view. Species illustrated are: *Dromaius novaehollandiae* (Palaeognathae); *Gallus gallus* (Galliformes); *Anas platyrhynchos* (Anseriformes); *Patagona gigas* (Strisores); *Tauraco erythrolophus* (Columbaves); *Fulica americana* (immature) / *F. atra* (adult; Gruiformes); *Fratercula arctica* (Charadriiformes); *Spheniscus demersus* (Phaethoquornithes); *Falco naumanni* (Telluraves). **B)** Colours and numbers on the phylogeny represent the nine subgroups compared in our investigation, following the topology of Prum et al. (2015)[22]. See Supplementary Data 9 for full information about the specimens investigated.

Figure 2. The morphology of the avian PPC and the landmark configuration used in this study. A) Ventral view of the skull of *Falco tinnunculus*, with the palatine and pterygoid highlighted in dark blue and dark purple, respectively (left). Detailed positions of the palatine and pterygoid landmarks on the *Falco tinnunculus* PPC (right). **B**) Overview of the morphological variation and the placement of the palatine and pterygoid landmarks in selected species belonging to various groups. See Supplementary Table 1 for detailed landmark positions.

Figure 3. Ontogenetic and phylogenetic variation of the PPC complex across birds. Principal Component Analysis (PCA), morphological disparity and pairwise group comparisons of pterygoid-palatinum complex (PPC) ontogenetic disparity across crown birds. A&B) PPC morphospace based on the first two principal components. C) Bar plot showing Procrustes variance per major subclade calculated using the function *morphol.disparity* from the R package geomoph[68]. The term "Mirando.&Charadriiformes" corresponds to Mirandornithes and

Charadriiformes. D) Correlation plot of pairwise distances between each subclade calculated using the function *procD.lm* from the R package geomoph[68], with stars indicating the levels of significance in each comparison (* = 0.05>P>0.01; ** =0.01>P>0.001; *** 0.001>P). For A, B and C, subclade colours follow Figure 1. In A, lines link immature and adult specimens of the same species; specific numbers in the PCA correspond to 1: *Ara ambiguus*; 2: *Lorius garrulus*; 3: *Cacatua alba*; 4: *Pteroglossus viridis*; 5: *Anorrhinus galeritus*; 6: *Podargus strigoides*; 7: *Phaethon lepturus*. See Supplementary Data 9 for detailed information on specimens. Reconstructions not to scale (A).

Figure 4. Ontogenetic and phylogenetic variation of palatine and pterygoid shape across birds. Principal Component Analysis (PCA) of palatine and pterygoid morphology. A) Palatine morphospace based on the first two PC scores. B) Pterygoid morphospace based on the first two PC scores. Subclade colours follow Figure 1. Circles indicate immature specimens and squares indicate adult specimens; each line links immatures and adults of the same species or same genus (the same genus was used in istances where the same species could not be sampled). Specific numbers in the PCA correspond to 1: *Ara ambiguus*; 2: *Lorius garrulus*; 3: *Cacatua alba*; 4: *Pteroglossus viridis*; 5: *Anorrhinus galeritus*; 6: *Podargus strigoides*; 7: *Phaethon lepturus*. See Supplementary Data 9 for detailed information on specimens. Reconstructions not to scale.

Figure 5. Morphological differences among groups in palatine and pterygoid ontogenetic shape changes. Morphological disparity and pairwise group comparisons by bone. Data for palatine in (A) and (B); data for pterygoid in (C) and (D). Bar plot showing Procrustes variance per avian subclade calculated using the function *morphol.disparity* from the R package geomoph[68] (A) and correlation plot of pairwise distances between each subgroup calculated using the function *procD.lm* from the R package geomoph[68], with asterisks indicating significance (* = 0.05>P>0.01; ** =0.01>P>0.001; *** 0.001>P) (B). Same plots are shown for the pterygoid (C and D). The term “Mirando.&Charadriiformes” corresponds to Mirandornithes and Charadriiformes. Subclade colours follow Figure 1. See Supplementary Data 3 for detailed results.

Figure 6. Pairwise angular comparisons across bird species within and between groups. A) Explanatory guide for interpreting the circular plot. **B)** Circular plot of inter-species angles within and between groups. Subclade colours follow Figure 1 for Palaeognathae, Galliformes, Anseriformes, Strisores, Columbaves, Gruiformes, Mirandornithes & Charadriiformes (Mirando. & Charadri.), Phaethoquornithes, and Telluraves. Specific colors correspond to intra-group angle calculations (i.e., angles between species within the same group), whereas grey color indicate inter-group angle comparisons (i.e. angles between species from different groups).

Figure 7. Pairwise divergence and convergence comparisons across bird species within and between groups. A) Explanatory guide for interpreting the frequency plot. **B)** Frequency plot of inter-species divergence/convergence values within and between groups. Subclade colours follow Figure 1 for Palaeognathae, Galliformes, Anseriformes, Strisores, Columbaves, Gruiformes, Mirandornithes & Charadriiformes (Mirando. & Charadri.), Phaethoquornithes, and Telluraves. Specific colors correspond to intra-group divergence/convergence calculations (i.e., divergence/convergence values between species within the same group), whereas grey color indicate inter-group divergence/convergence calculations (i.e., divergence/convergence values between species from different groups).

Figure 8. The altricial-precocial spectrum and its effects on ontogenetic variation in the avian bony palate. A) Plot of Chick PC1 (Ducatez and Field (2021)[32]) across avian phylogeny (left). Ancestral states (node values) across the phylogeny were reconstructed using the contMap function from the R package phytools (Revell 2012[82]). Chick PC1 corresponds to the first axis of the PCA performed on a matrix of seven discrete developmental traits (hatchling down coverage, hatchling eye condition, age at eye opening, hatchling locomotor activity, hatchling feeding capacity, ratio of time spent in the nest to age at first flight, and post-nest behavior), capturing the atricial-precocial spectrum (Ducatez and Field (2021)[32]). B) Circular plot of inter-species angles and C) Frequency plot of inter-species divergence/convergence relative to developmental mode categories.

Figure 9. Covariation in developmental mode and ontogeny of the PPC may be the result of a few evolutionary events early in crown bird evolutionary history. A) Schematic representation of the relationship between two trait values across phylogenetic groups, results from PGLS and OLS models and their underlying evolutionary meaning (modified from Clauss et al., 2013). **B)** Distance map between immature and adult (left), angle (middle) and divergence-convergence (right) values between individual species and estimated ancestral state as a reference value (see Materials and Methods) across avian phylogeny using contMap function from the R package phytools (Revell 2012[82]). Circular lines in different shades of gray represent the nine avian subclades under investigation; see Figure 1. Tables under each phylogenetic tree indicate statistical results of OLS and PGLS regressions between ontogenetic parameters and developmental mode (Chick PC1). **C)** Plot of the OLS regression (black line) between immature-adult distances (left), angles (centre), and divergence-convergence (right) values and Chick PC1 values.

Editorial Summary:

By studying how the bird palate develops after hatching across many bird groups, this study shows that differences among major bird lineages are shaped by both evolutionary history and developmental mode.

Peer Review Information: *Nature Communications* thanks Sander Gussekloo and the other anonymous, reviewer(s) for their contribution to the peer review of this work. A peer review file is available."

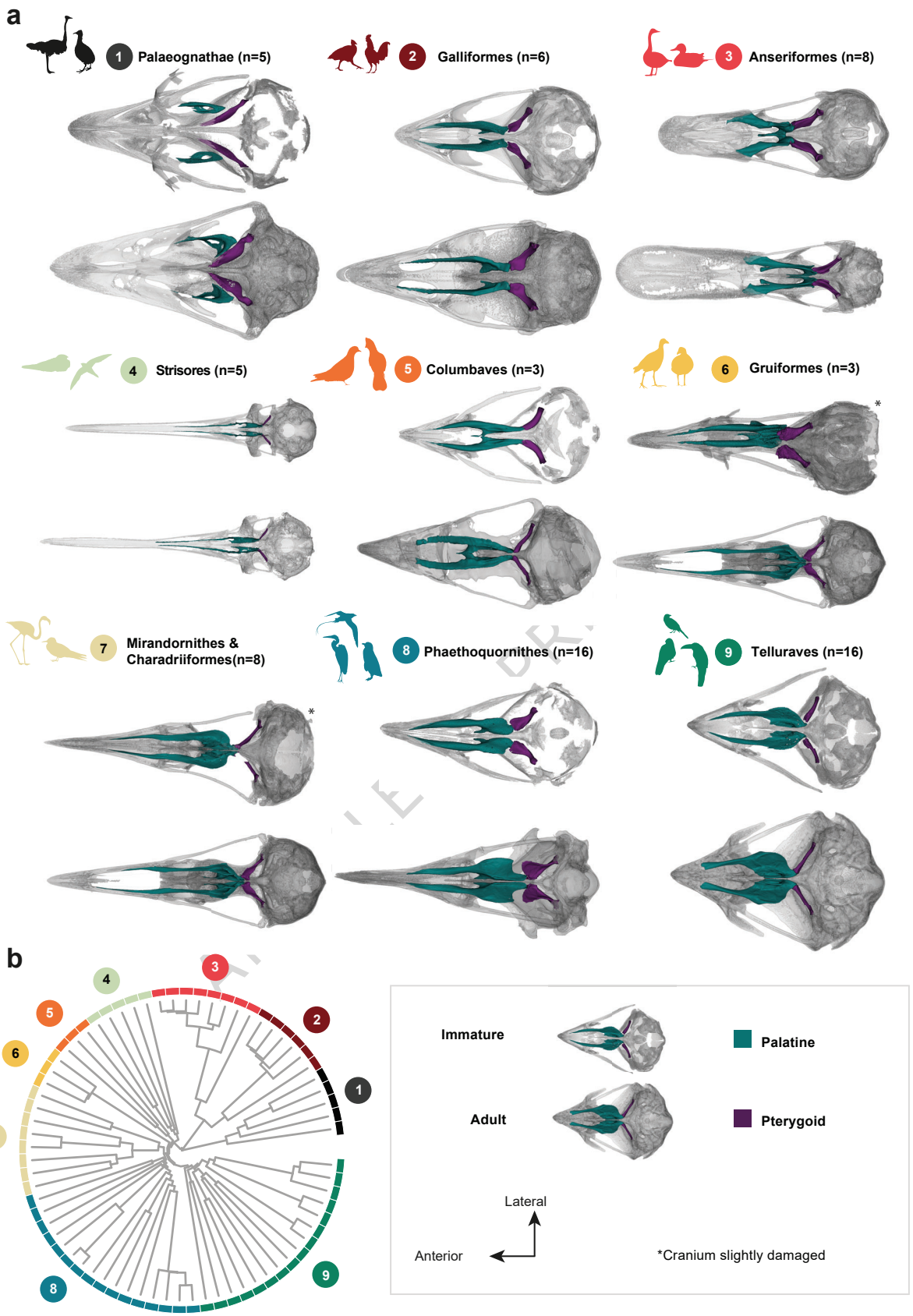
a
1 Palaeognathae (n=5)
2 Galliformes (n=6)
3 Anseriformes (n=8)
4 Strisores (n=5)
5 Columbaves (n=3)
6 Gruiformes (n=3)
7 Mirandornithes & Charadriiformes(n=8)
8 Phaethoquornithes (n=16)
9 Telluraves (n=16)
*
b
Immature
Adult
Palatine
Pterygoid
Lateral
Anterior
*Cranium slightly damaged

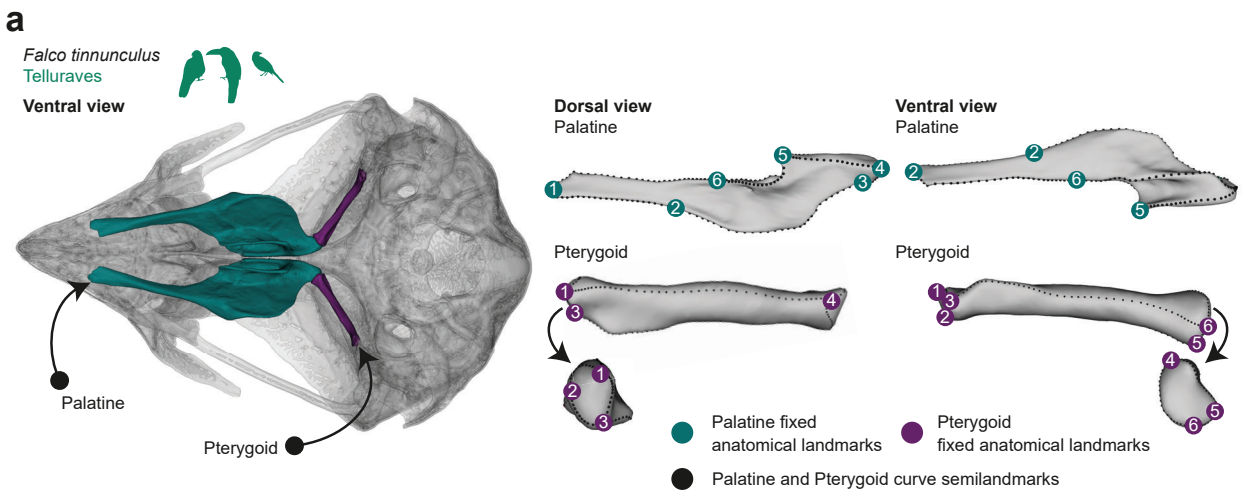

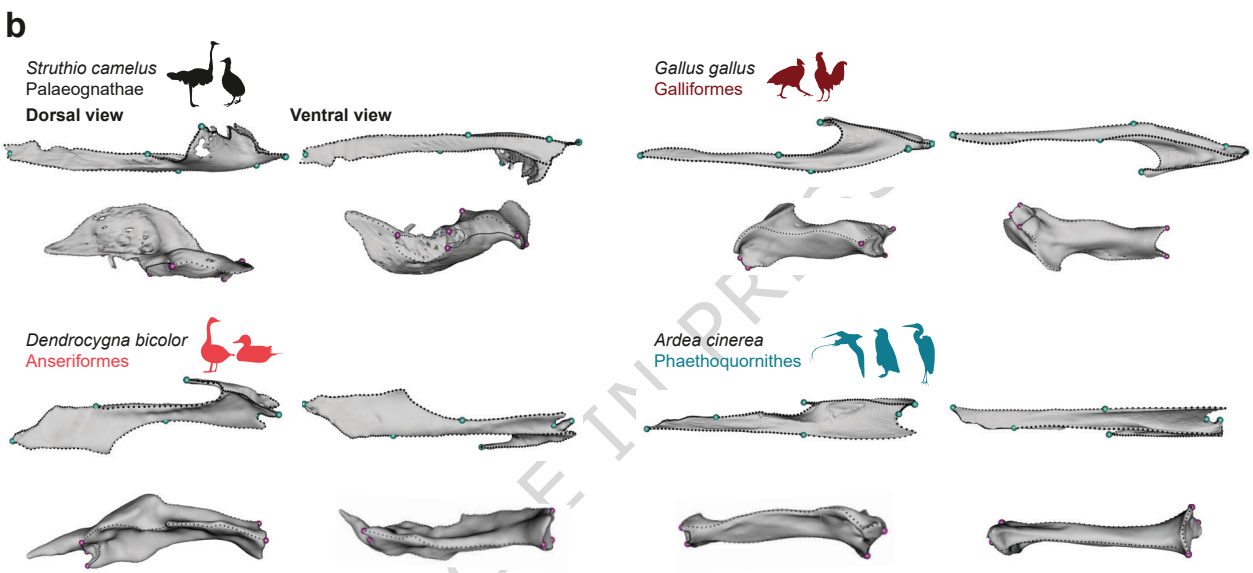

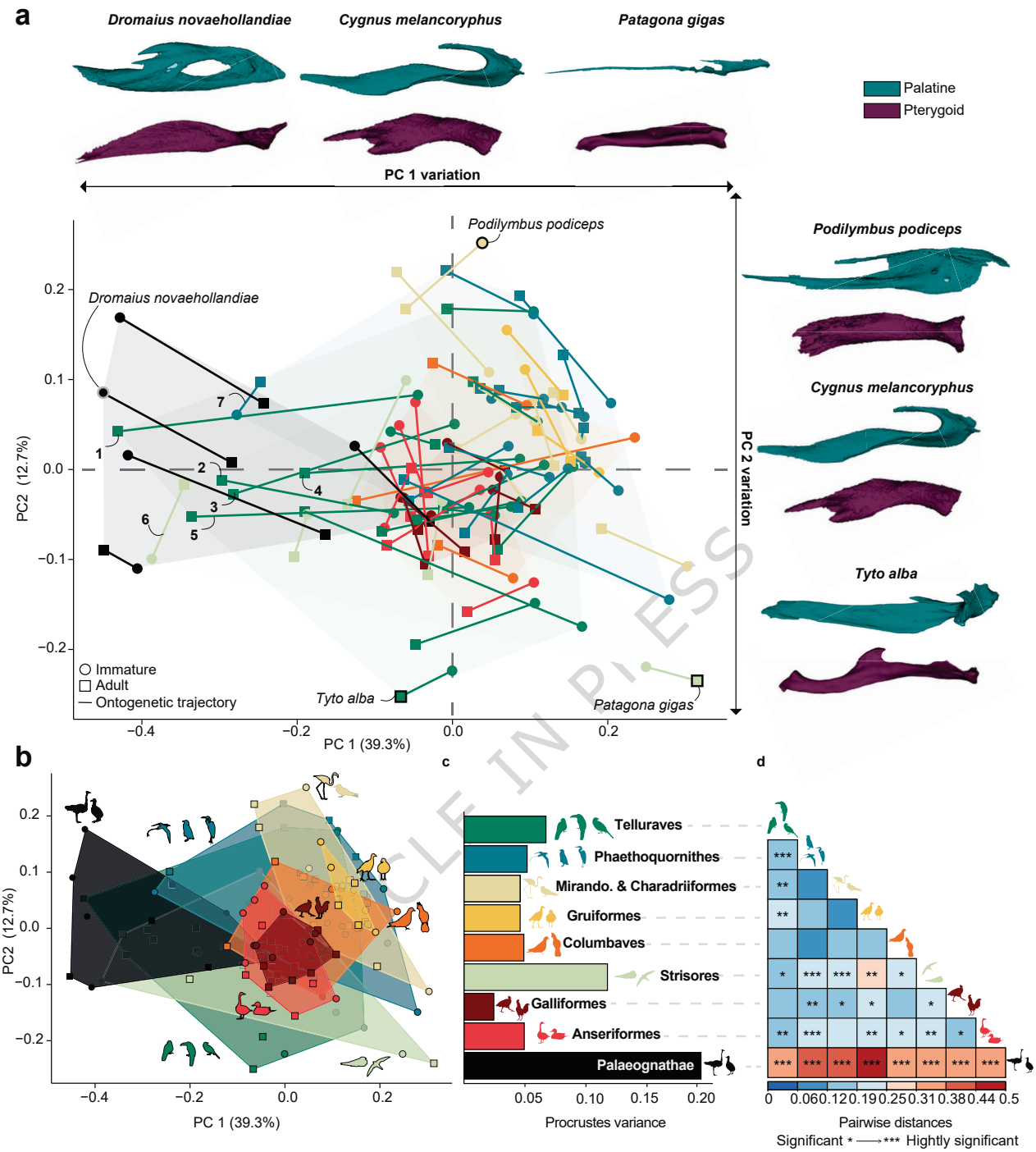
a
Dromaius novaehollandiae
Cygnus melancoryphus
Patagona gigas
Palatine
Pterygoid
PC 1 variation
Podilymbus podiceps
Dromaius novaehollandiae
PC2 (12.7%)
PC 2 variation
PC 1 (39.3%)
Immature
Adult
Ontogenetic trajectory
Tyto alba
Patagona gigas
Podilymbus podiceps
Cygnus melancoryphus
Tyto alba
b
c
d
PC2 (12.7%)
PC 1 (39.3%)
Telluraves
Phaethoquornithes
Mirando. & Charadriiformes
Gruiformes
Columbaves
Strisores
Galliformes
Anseriformes
Palaeognathae
Procrustes variance
Pairwise distances
Significant * ⟶ *** Hightly significant

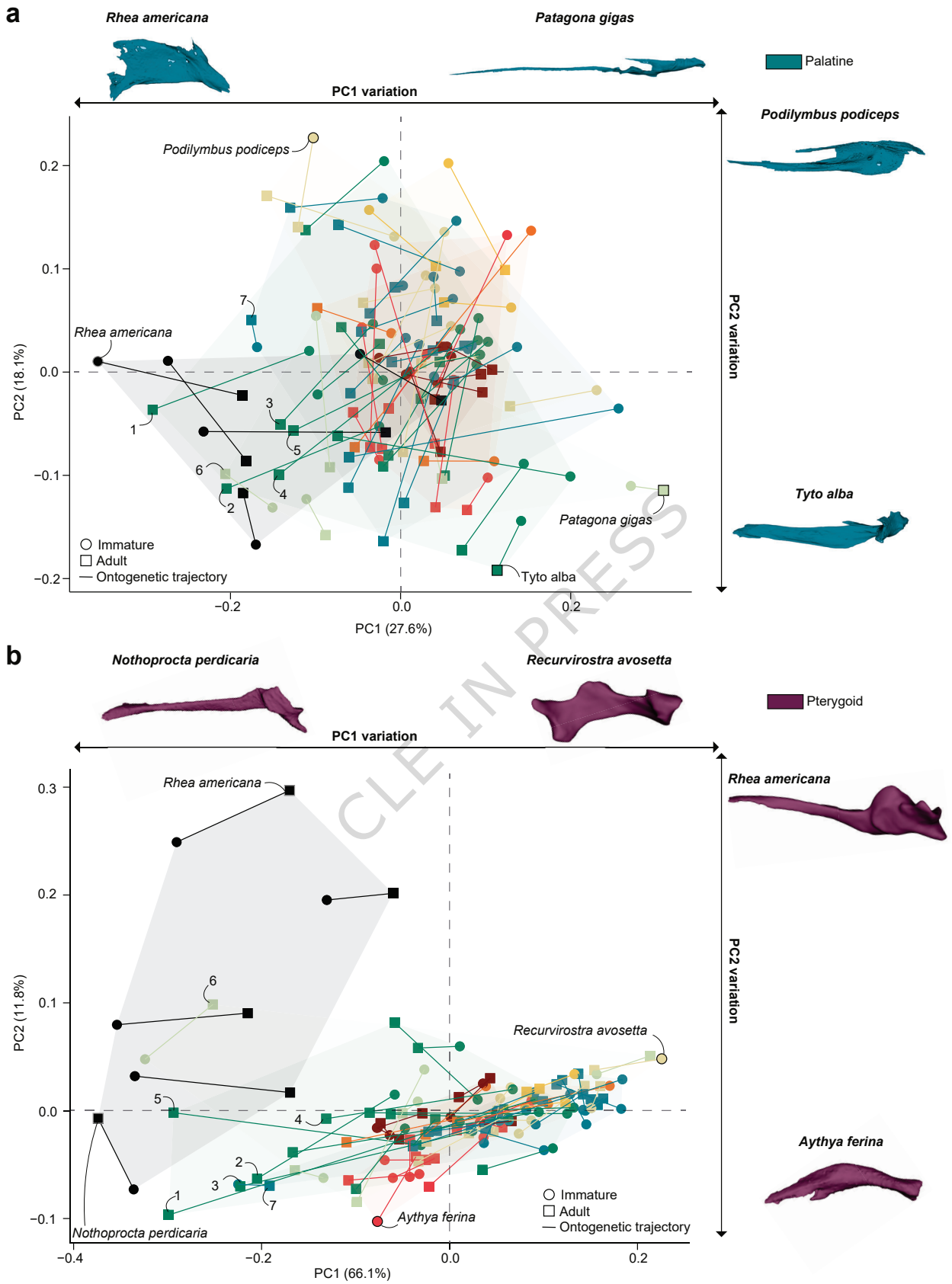
a
Rhea americana
Patagona gigas
Palatine
PC1 variation
Podilymbus podiceps
Podilymbus podiceps
PC2 variation
Rhea americana
Tyto alba
Patagona gigas
Immature
Adult
Ontogenetic trajectory
Tyto alba
PC2 (18.1%)
PC1 (27.6%)
b
Nothoprocta perdicaria
Recurvirostra avosetta
Pterygoid
PC1 variation
Rhea americana
Rhea americana
PC2 variation
Recurvirostra avosetta
Aythya ferina
Immature
Adult
Ontogenetic trajectory
Nothoprocta perdicaria
PC2 (11.8%)
PC1 (66.1%)

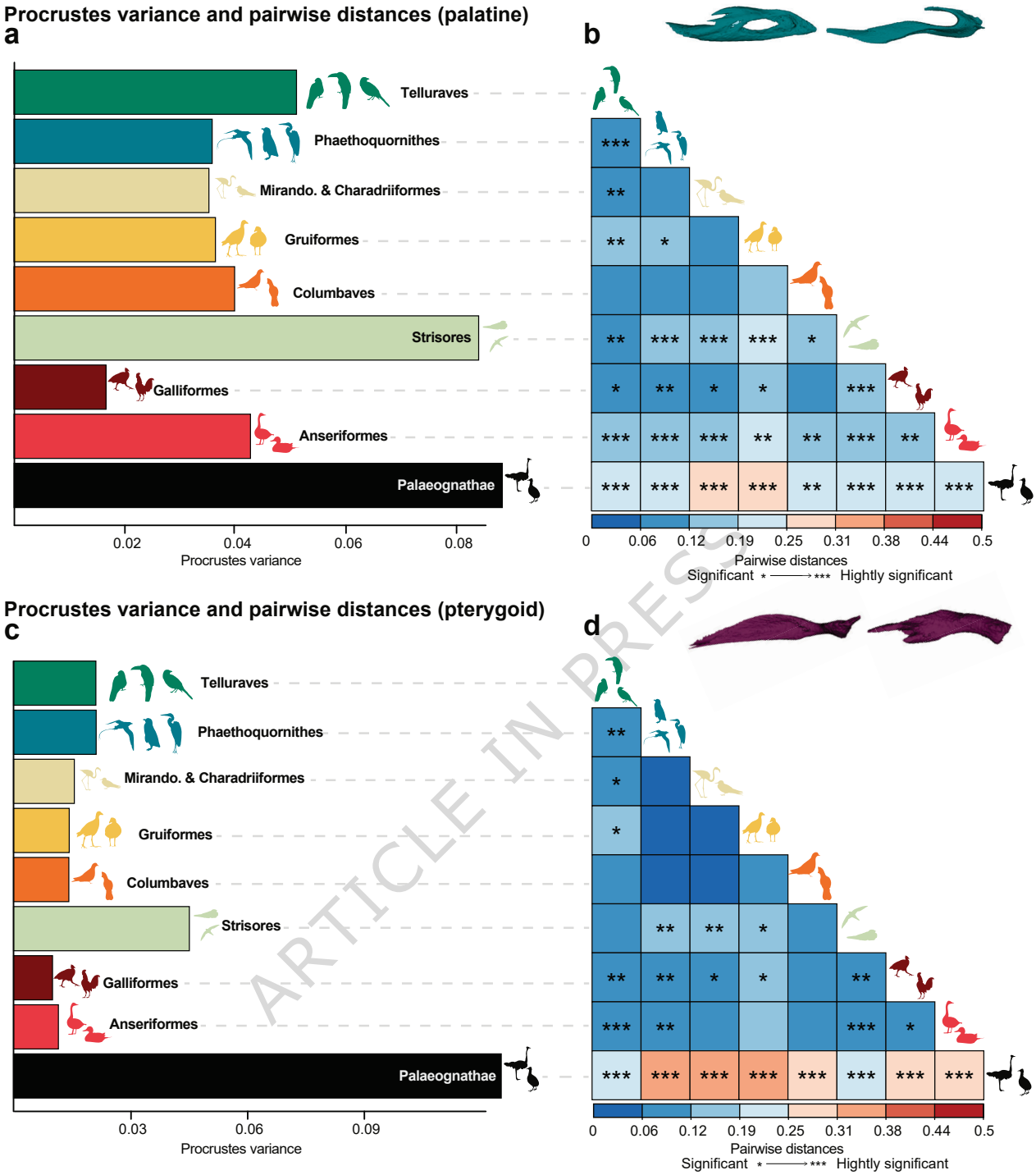

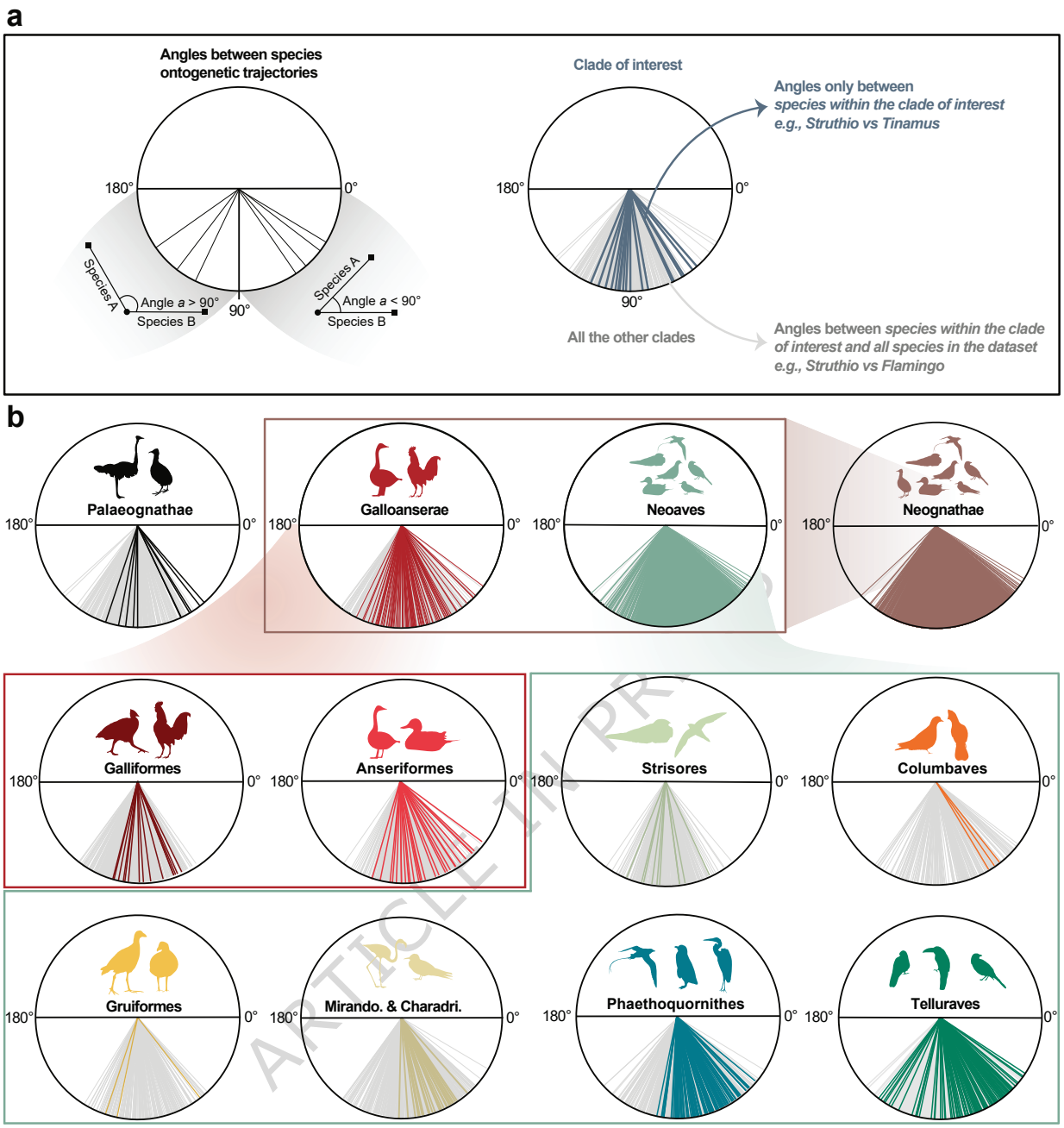
a
Angles between species ontogenetic trajectories
180°
0°
90°
Species A
Species B
Angle a > 90°
Angle a < 90°
Clade of interest
Angles only between species within the clade of interest e.g., Struthio vs Tinamus
All the other clades
Angles between species within the clade of interest and all species in the dataset e.g., Struthio vs Flamingo
b
Palaeognathae
Galloanserae
Neoaves
Neognathae
Galliformes
Anseriformes
Strisores
Columbaves
Gruiformes
Mirando. & Charadri.
Phaethoquornithes
Telluraves